



Metrological needs and reliable solutions for optics fabrication related to E-ELT

M. M. Civitani, G. Sironi, M. Ghigo, G. Vecchi, and M. Riva

Istituto Nazionale di Astrofisica – Osservatorio Astronomico di Brera, Via Bianchi 46, I-23807 Merate, Italy, e-mail: marta.civitani@brera.inaf.it

Abstract. In order to contribute and support the R&D activities related to the E-ELT (European Extremely Large Telescope) program, the INAF-OAB acquired a dedicated robotic polisher machine, the IRP1200 by Zeeko. It will be used in synergy with the ion beam figuring technique, already available at OAB for the realization of prototypes and advanced optical components, as the optics of the Multi-conjugate Adaptive Optics Relay module (MAORY). In this paper, starting from the discussion of the metrological needs to be fulfilled during the different parts of the machining for the different kind of optics, we define the metrological scheme that will be followed. Moreover, we present the concept for a new measurement machine based of non-contact scanning probes, capable of nanometer uncertainty and compatible with the optics design to be realized.

Key words. European Extremely Large Telescope (E-ELT) – MAORY – segment metrology – Measurement machine – Profilometer – null sensor

1. Introduction

In order to allow a rapid optics manufacturing process, a precise and accurate metrological technique is needed. Moreover, a versatile tool, which can be used since the grinding phase of the optic to the end of the polishing process, it is highly desirable to guide efficient fabrication. During last years different profilometers have been designed and realized but are in general tailored on specific mirror designs (Bos et al. 2014). This is a huge limiting factor for a cutting edge optics manufacturing laboratory, like the one that is being created at INAF-OAB in the framework of the R&D activities related to the E-ELT (European Extremely Large Telescope) program funded with 'T-Rex premiale' program. Here new and attractive free form optics can be realized start-

ing from innovative optical design: the finalization of the large Ion beam facility and the purchase of the dedicated robotic polisher machine, the IRP1200 by Zeeko allow the manufacturing of prototypes and advanced optical components up to few nanometers accuracy. The figuring performances of the Large Ion Beam Facility has been recently proven on a prototypal segment for E-ELT primary mirror (Ghigo et al. 2014). On the other hand, the commissioning of the IRP1200 by Zeeko is in progress (Vecchi et al. 2015). In this context, an adequate metrological device is of fundamental importance for a complete production chain. A profilometer can accomplish this task. If properly designed, it may be used for a wide range of optics both concave and convex, both spheric and aspheric mirrors, fulfilling the flex-

ibility requirement of the laboratory. In this paper we present the conceptual design for a new hybrid profilometer/deflectometer system as an accurate method for rapid metrology of freeform optical surfaces.

2. Conceptual design

The proposed metrological device relies on two different approaches, joint together to get the more accurate and fast measure of the surface under test. It combines the proven approach of the measure with respect to a reference with the null sensor technique (Civitani et al. 2010) (Sironi et al. 2010) and the deflectometric approach. On one side, the traditional scanning approach is necessary to overcome all the systematics that can arise from the alignment errors, not measurable in the deflectometric set-up in view of few nanometers accuracy. On the other hand the deflectometric approach allows the high sensitivity on mid-high frequency errors, that would need time consuming procedures to be sampled by a profilometer. The required accuracy of the overall metrological device is $10nm$ rms, on a surface of $1400mm \times 1400mm$ and a total sag of $30mm$. These limits are derived considering the geometry of the E-ELT segments and the one of the MAORY optics elements (Diolaiti et al. 2014). These last items, having smaller radius of curvature, pose tighter constraints in the design.

2.1. Profilometer set-up

The null-sensor measuring principle works acquiring the distance along a line of points (direction X) of the surface under test from a rigid reference bar, consisting in a optically-polished Zerodur reference flat in Fig. 1. The displacement of the sample along the orthogonal direction Y allows the composition of the mesh grid of point on the sample surface. If the probe position along the measurement direction is known, the obtained lines can be stitched together to obtain a 3D reconstruction of the surface form. The residuals with respect to the theoretical surface are then derived fitting the overall set of data.

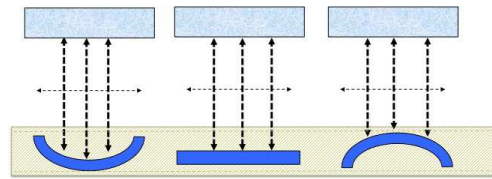


Fig. 1. The measurement of the surface is derived from the measure of the cavity between a reference and the mirror to be measured that can be convex, flat and concave.

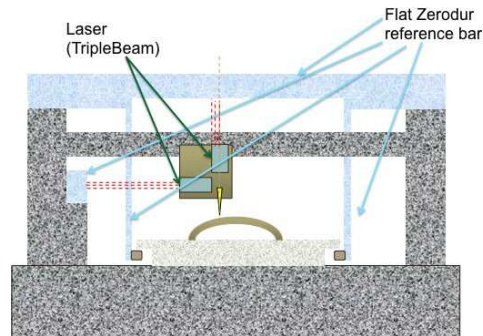


Fig. 2. Front view of the metrological machine

The precise measurement of the cavity between the surface and the reference is obtained by means of two sensors, mounted on the same stage measuring in opposite directions. See Fig. 2. An optical probe is highly useful in the first part of the polishing process, with a higher material removal rate, to figure the surface rapidly and precisely. Depending on the amplitude of the field of view of this sensor, its alignment with respect to the surface can be avoided. The CHRcodile sensor head, already experienced on the CUP profilometer, is a possible choice. It is based on a lens that deliberately suffers of chromatic aberration. The sensor currently available at OAB has a range of $660microns$, is characterized by $20nm$ vertical resolution and $2microns$ lateral resolution. The sensor noise is related to the working range of the sensor head and can be reduced up to $3nm$ rms for the CHR100. In order to overcome the limited measuring range of the optical sensor (insufficient when a curved profile with a large sag is measured), the CHRcodile is used in null sensor configuration. A trans-

Table 1. Achieved performances on different sample geometries

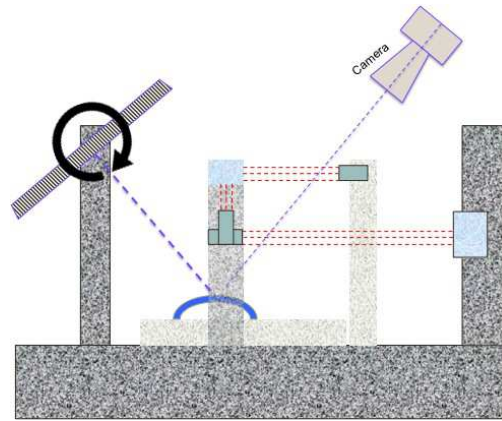
Item #	Flat 10		Cylindrical		Spherical	
	PtV [nm]	Rms [nm]	PtV [nm]	Rms [nm]	PtV [nm]	Spherical rms [nm]
Yaw	2.4	0.4	5.6	1.6	5.2	1.1
Pitch	< 0.1	< 0.1	< 0.1	< 0.1	7.8	1.4
Out-of-Straightness X	26.3	7.1	24.6	3.1	24.8	3.1
Out-of-Straightness Y	< 0.1	< 0.1	< 0.1	< 0.1	17.3	2.1
All	26.7	6.8	23.9	3.4	39.1	4.3

lational stage moving in Z direction keeps the surface continuously in the centre of the CHR measuring range avoiding the problems of non-linearity at the edges of its measurement range.

On the opposite side of the Z translation stage, a laser interferometer is measuring the distance from the reference bar. The triple beam interferometer (SIOS, model SP 2000-TR11) is based on three laser pencil beams to measure distances and tilts with respect to a reference surface. The maximum allowed tilt is $2'$. The linear and angular resolutions are $1nm$ and of $0.02''$ respectively. It is already in use on the CUP profilometer and the noise in the measurement is around $5nm$ rms.

The accuracy and the precision of the profilometer rely on the precision of the sensors but also on the accuracy in the positioning the sensor and the stability in temperature of the reference system.

With respect to the X-Y stage movement accuracy, a general assessment on the stages requirement performances has been achieved through simulations. Assuming a distance of $500mm$ between a reference and the surface under test, which maximum size is $1400mm \times 1400mm$, the possible carriages errors have been varied and a measurement results simulated. For geometric reasons they are mainly prone to yaw and pitch rotations and straightness along X and Y direction. Three different surface shapes have been considered: a flat with an angle of $15deg$ with respect to the measuring direction, a spherical surface and a cylindrical surface with radius of curvature of $5m$. The selection of these items is in line with the geometry of the optics involved in E-ELT project. The sensitivity with respect to the dif-

**Fig. 3.** Side view of the new metrological device.

ferent stage errors has been derived simulating the acquisition of data points: each one of these errors introduces a systematic in the measurement. Its value is given in terms of rms of the measured data with respect to the theoretical one. The results are summarized in Table 1. For each case, the rms and the PtV are given. In the last line the general case in which all the errors are combined is reported. In those cases, the maximum amplitude for the yaw and pitch errors is $0.04''$, while the out of straightness in X and Y direction is respectively $150nm$ and $115nm$.

Even foreseeing air bearing stages, these numbers are difficult to reach and an additional piezo stage is used to compensate residual deviation and rotations with respect to a fixed system reference. This piezo stage works in closed loop on metrological data acquired with laser pointing in orthogonal directions in order to bring the sensors head in the desired posi-

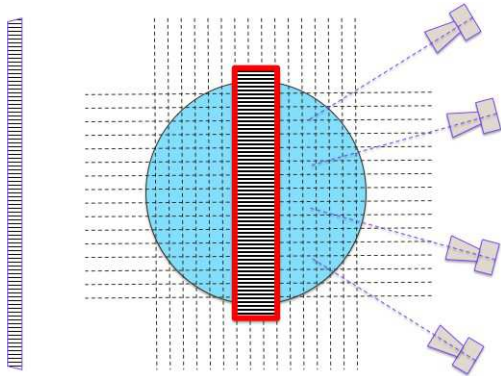


Fig. 4. Top view of the new metrological device.

tion with respect to the sample to be measured, in such a way to fulfill the Abbe condition. Additional Zerodur reference bars are added in order to have a fixed reference system to be assumed for the correction. In order to maintain the dimension of the cavity as stable as possible and to guarantee the best environmental condition for the lasers, the chamber thermal control should be better than 0.2C. Capacitive sensors are foreseen to control the distance between the reference bar and the supporting stage, therefore controlling the vertical size of the cavity. They are mounted on Zerodur support to control the variations in amplitude due to the temperature. They also guarantee that the movements of the surface under measurement due to the out of flatness of the Y stages are known and can be taken into account in data post-processing.

2.2. Deflectometry set-up

A schematic diagram illustrating the metrological device concept is shown in Fig. 3 and in Fig. 4. The different parts (monitor and cameras) are located in the system so that the measured area correspond to the central area under the reference bar. In this way the profilometer data can be used to improve the post-processing of the deflectometric data. A monitor is used to create a sinusoidal pattern in pixel intensity that is reflected from the central area of the mirror under test. The reflected rays propagate toward the cameras displaced

in such a way to image all the test surface so that each local area of surface corresponds to a pixel in one camera, with a slight overlapping of the camera fields. Through the analysis of the reflected pattern, it is possible to directly calculate the local slopes of the test surface and obtain the surface height with integration. Further details are given in Sironi et al. (2014)

3. Conclusions

We have presented a new metrological machine based on the combination of a deflectometric approach and of the more traditional profilometer measure with respect to a reference bar. We use deflectometry to make direct measurements of local slopes and rapidly provide highly accurate surface profiles of optical surfaces at mid and high frequencies while the low frequency profiles errors are sampled with the scanning probe. The machine can achieve an accuracy of nearly 10nm rms with high spatial resolution, with large dynamic range (e.g., 30mm freeform departure) and large measurement area of 1.4m x 1.4m in size or more. Thanks to the implementation of the deflectometry approach, the total measurement time is maintained short even if with a scanning high sampling of fractions of millimeters in both direction is guaranteed. The performances of the system have been inferred through simulations and confirmed with the experience made on prototypal metrological devices working with the same approach.

References

- Bos, A., et al. 2014, Proc. SPIE, 9151, 91510X
- Civitani, M.M., et al. 2010, Proc. SPIE, 7803,78030L
- Diolaiti, E., et al. 2014, Proc. SPIE, 9148, 91480Y
- Ghigo, M., et al. 2014, Proc. SPIE, 9151, 91510Q
- Sironi, G., et al. 2011, Proc. SPIE, 8147, 814718
- Sironi, G., et al. 2013, Proc. SPIE, 9151, 91510T
- Vecchi, G., et al. 2015, MmSAI, 86, 408